Nuclear Matrix Elements for $0\nu\beta\beta$ Decay: Progress and Prospects

Jiangming Yao (尧江明)

Sun Yat-sen University (中山大学)

第一届中微子散射：理论、实验、唯象研讨会
2024年5月18日，国科大杭州高等研究院

Outline

1. Introduction
2. Modeling nuclear matrix elements of $0\nu\beta\beta$ decay in the standard mechanism
   - with phenomenological operators: correlation relations and UQ
   - with operators from chiral EFT
3. Neutrinoless double-beta decay in non-standard mechanisms
   - Recent progress in MR-CDFT plus chiral EFT transition operators
4. Summary and prospects

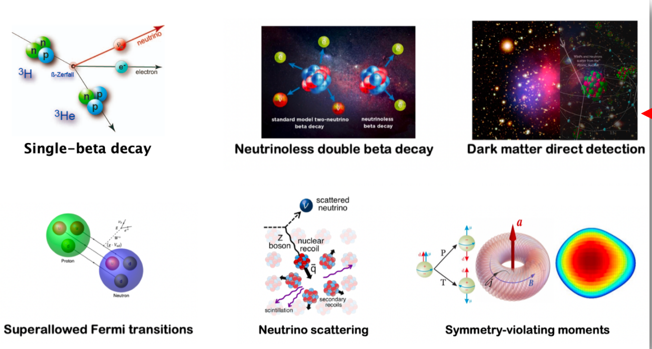

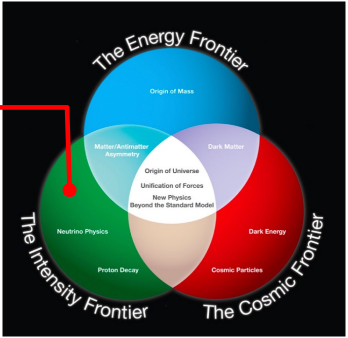

- Frontiers in physics
- Testing fundamental symmetries and interactions.

- Low-energy probes
- Requiring accurate nuclear matrix elements

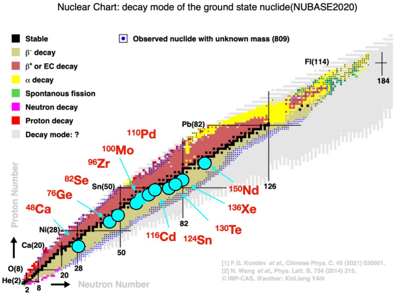

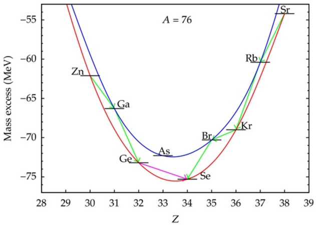

- The two modes of $\beta^-\beta^-$ decay:

  Goeppert-Mayer (1935); Furry (1939)

$$(A, Z) \to (A, Z+2) + 2e^- + (2\bar{\nu}_e)$$

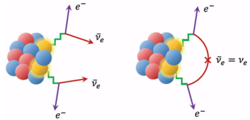

- Kinetic energy spectrum of electrons

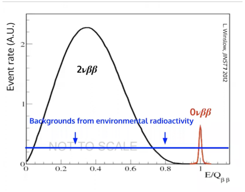

Status of measurements on $0\nu\beta\beta$ decay

Isotope	$G_{0\nu}$ $[10^{-14}\ \text{yr}^{-1}]$	$M^{0\nu}$ [min, max]	$T_{1/2}^{0\nu}$ [yr]	$\langle m_{\beta\beta}\rangle$ [meV]	Experiments References
^{48}Ca	2.48	[0.85, 2.94]	$> 5.8 \cdot 10^{22}$	[2841, 9828]	CANDLES: PRC78, 058501 (2008)
^{76}Ge	0.24	[2.38, 6.64]	$> 1.8 \cdot 10^{26}$	[73, 204]	GERDA: PRL125, 252502(2020)
^{82}Se	1.01	[2.72, 5.30]	$> 4.6 \cdot 10^{24}$	[277, 540]	CUPID-0: PRL129, 111801 (2023)
^{96}Zr	2.06	[2.86, 6.47]	$> 9.2 \cdot 10^{21}$	[3557, 8047]	NPA847, 168 (2010)
^{100}Mo	1.59	[3.84, 6.59]	$> 1.5 \cdot 10^{24}$	[310, 540]	CUPID-Mo: PRL126, 181802(2021)
^{116}Cd	0.48	[3.29, 5.52]	$> 2.2 \cdot 10^{23}$	[1766, 2963]	PRD 98, 092007 (2018)
^{130}Te	1.42	[1.37, 6.41]	$> 2.2 \cdot 10^{25}$	[88, 413]	CUORE: Nature 604, 53(2022)
^{136}Xe	1.46	[1.11, 4.77]	$> 2.3 \cdot 10^{26}$	[36, 156]	KamLAND-Zen: PRL130, 051801(2023)
^{150}Nd	6.30	[1.71, 5.60]	$> 2.0 \cdot 10^{22}$	[1593, 5219]	NEMO-3: PRD 94, 072003 (2016)

Note: $g_A = 1.27$, $G_{0\nu}$ is taken from J. Kotila and F. Iachello, Phys. Rev. C 85, 034316 (2012)

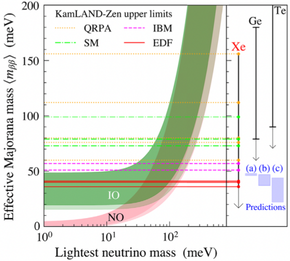

In the standard mechanism, the effective neutrino mass

$$\langle m_{\beta\beta}\rangle = \sum_i U_{ei}^2 m_i = \left[\frac{m_e^2}{g_A^4 G_{0\nu} T_{1/2}^{0\nu} |M^{0\nu}|^2}\right]^{1/2}$$

- For the IO: $\langle m_{\beta\beta}\rangle \in [18, 50]\ \text{meV}$.
- An uncertainty of a factor of about 3 or even more.

Next-generation of experiments

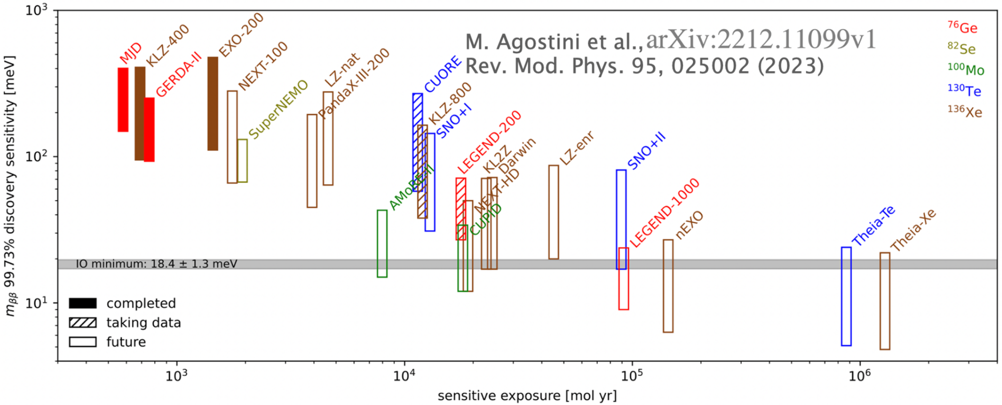

- Lifetime sensitivity of the ton-scale experiments: $> 10^{28}$yr.
- Whether or not the ton-scale experiments are able to cover the entire parameter space for the IO case depends strongly on the employed NME.

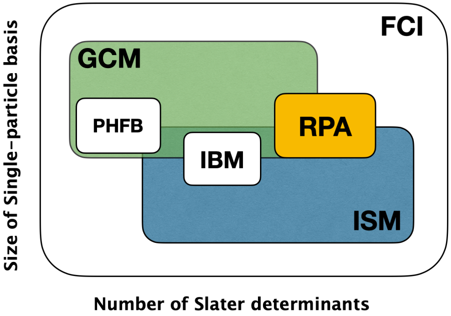

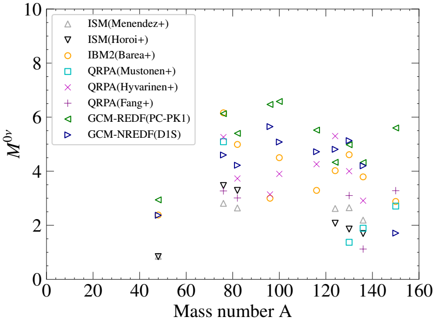

JMY, J. Meng, Y.F. Niu, P. Ring, PPNP 126, 103965 (2022)

- Discrepancy is about a factor of 3 or even larger.
- Efforts in resolving the discrepancy: improve models, examine correlation relations.
- Uncertainty quantification is required to claim precision: statistical (fluctuation in input parameters) and systematic (model approximations) errors.

Correlation relations: NLDBD v.s. DGT

- The NME for the ground-state to ground-state double Gamow-Teller (DGT) transition

$$M^{\mathrm{DGT}} = \left\langle 0_f^+ \left| \sum_{1,2} [\sigma_1 \otimes \sigma_2]^0 \tau_1^+ \tau_2^+ \right| 0_i^+ \right\rangle$$

No neutrino potential and no intermediate states.

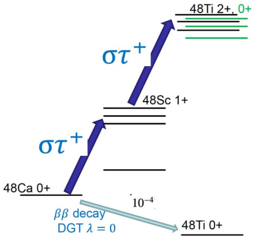

- The correlation relation between the NMEs of $0\nu\beta\beta$-decay and DGT holds for ISM, EDF, and IBM2 models, but not for QRPA,

$$M^{0\nu} A^{-1/6} = a M^{\mathrm{DGT}} + b.$$

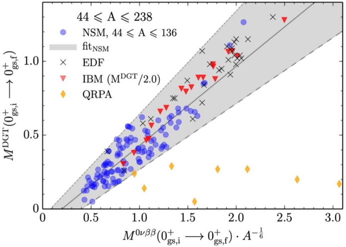

N. Shimizu et al., PRL120, 142502 (2018); C. Barase et al., PRC106, 034309 (2022)

Correlation relations: NLDBD v.s. DGT in QRPA

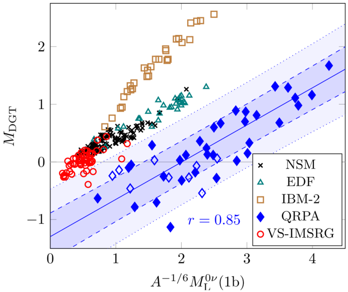

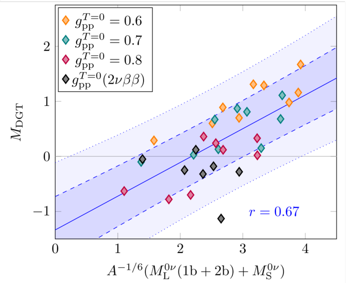

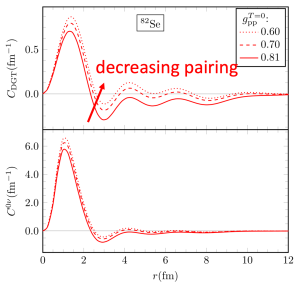

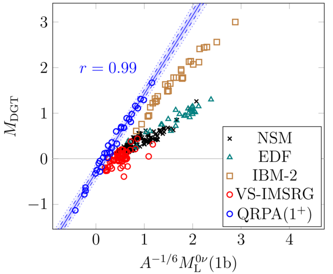

- Correlation between the DGT and NLDBD is weaker in the QRPA results
- The weak correlation is due to the strong cancellation between the long-range and short-range contributions.
- The correlation becomes much stronger in the QRPA if only including the contribution of M0v (1+)
- Many-body correlations affect the cancellation in the NME of DGT.

L. Jokiniemi, J. Menéndez, PRC107, 044316 (2023)

Correlation relations: NLDBD v.s. DGT

- Correlation between the NLDBD and DGT in the candidate nuclei from Relativistic Configuration-interaction Density functional theory.
- No cancellation from the long-range contribution leads to a strong correlation.

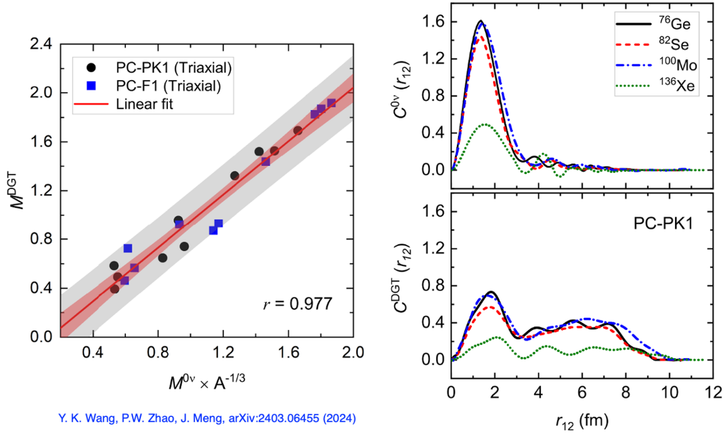

Y. K. Wang, P.W. Zhao, J. Meng, arXiv:2403.06455 (2024)

- Starting from three different shell-model Hamiltonians.
- 10^3 samples with each of the two-body interaction matrix elements of the original shell-model Hamiltonian changing within the range of 10%.
- Correlation relation is examined with the Pearson coefficient

$$r = \frac{\sum (x_i - \bar{x})(y_i - \bar{y})}{\sqrt{\sum (x_i - \bar{x})^2 \sum (y_i - \bar{y})^2}}.$$

- $M^{0\nu}$ is strongly correlated with $M^{2\nu}$, the excitation energies of $2_1^+, 4_1^+, 6_1^+$ states in both parent (P) and daughter (D) nuclei.

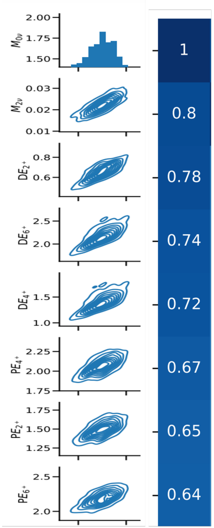

M. M. Horoi, A. Neacsu, S. Stoica, PRC107, 045501 (2023)

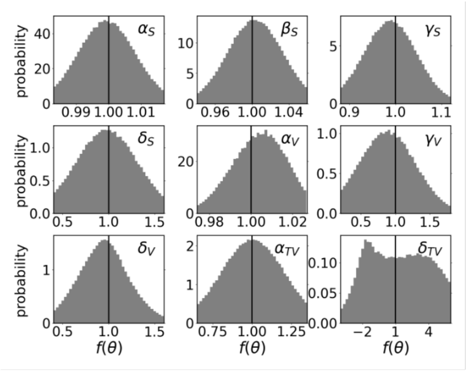

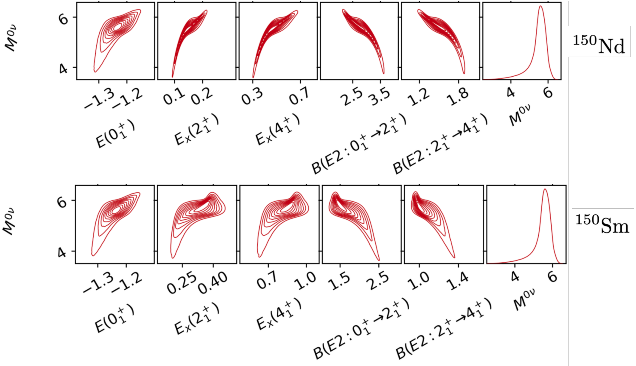

- 9 parameters $(\alpha_S, \beta_S, \gamma_S, \delta_S, \alpha_V, \gamma_V, \delta_V, \alpha_{TV}, \delta_{TV})$ in the relativistic EDF.
- 32 training EDFs $E(c_i)$ and 32 test EDFs $E(c_t)$.
- Implementation of eigenvector continuation (EC) method to emulate 10^6 times of MR-CDFT calculations (sampling EDFs around PC-PK1, corresponding $f(\theta) = 1$).

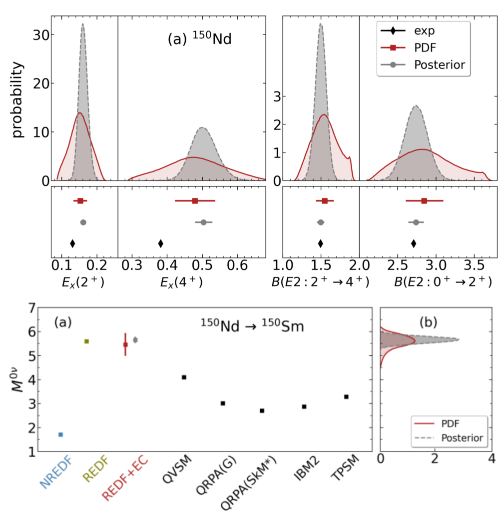

- The probability distribution function (pdf) is largely overlapping with the posterior distribution derived using the Bayesian method based on the correlation relation between the $M^{0\nu}$ and $B(E2:0_1^+\to 2_1^+)$ of ^{150}Nd, with $r=-0.90$.
- The obtained $M^{0\nu}=5.65\pm0.14$, compared to the previous value 5.60.

  JMY, Song, Hagino, Ring, Meng, PRC91, 024316 (2015).
- The main discrepancy among different models is originated from the systematic error, which is difficult to reduce.

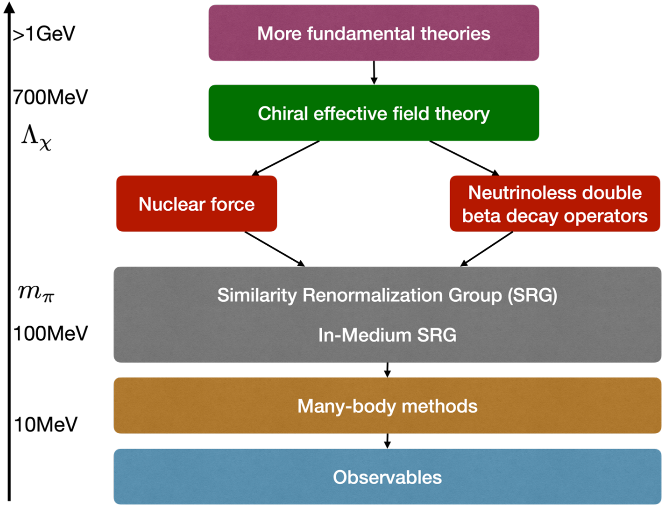

The basic idea of current efforts:

- Construct an EFT at the nuclear energy scale in terms of $N, \pi, (e, \nu)$ dofs.
- Match the EFT to more fundamental theories at higher-energy scales with the renormalization group (difficult for nuclear force)
- Identify the relevant (chiral) symmetries, and write down all possible contributions according to a power counting rule, $(m_\pi, Q)/\Lambda_\chi$.

- At $E \sim 100$ MeV: operators are expressed in terms of nucleons, pions, and leptons, arranged in the order $[(Q, m_\pi)/\Lambda_\chi]^\nu$,

$$\nu = 2A + 2L - 2 + \sum_i (\frac{n_f}{2} + d - 2 + n_e)_i$$

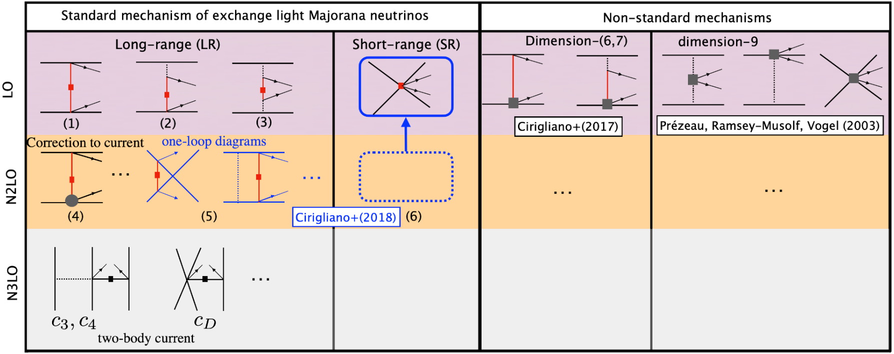

Ab initio methods for the lightest candidate ^{48}Ca

- Multi-reference in-medium generator coordinate method (IM-GCM)

  JMY et al., PRL124, 232501 (2020)

- IMSRG+ISM (VS-IMSRG)

  A. Belley et al., PRL126, 042502 (2021)

- Coupled-cluster with singlets, doublets, and partial triplets (CCSDT1) .

  S. Novario et al., PRL126, 182502 (2021)

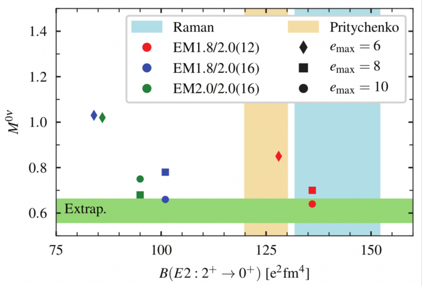

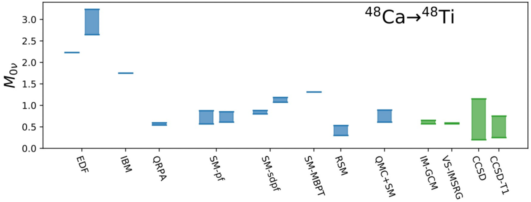

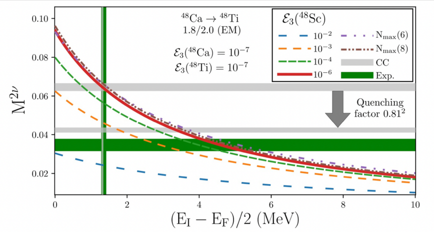

- Introducing a contact transition operator to ensure renormalizability at LO V. Cirigliano et al., PRL120, 202001 (2018)

$$O_S^{0\nu} = -2 g_\nu^{NN} \tau^{(1)+} \tau^{(2)+}$$

- Predicted the transition amplitude $2n \to 2p + 2e^-$,

$$\mathcal{A}_\nu(25\mathrm{MeV}, 30\mathrm{MeV}) \simeq -0.0195(5)\mathrm{MeV}^{-2},$$

serving as synthetic datum. V. Cirigliano et al., PRL126, 172002 (2021)

- We determine the LEC g_ν^{NN} consistent with different nuclear forces based on the synthetic data.
- The contact term turns out to enhance the NME for ^{48}Ca by 43(7)%, thus halves the half-life.

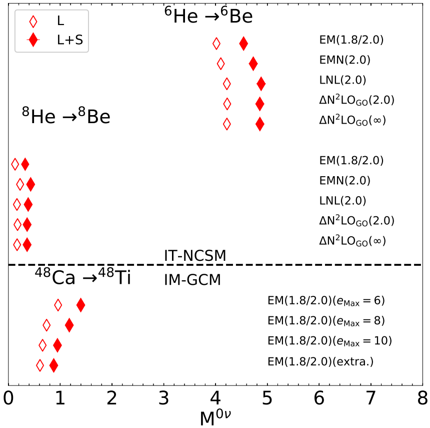

R. Wirth, JMY, H. Hergert, PRL127, 242502 (2021)

- Examine the correlation relation with three different ab initio methods.

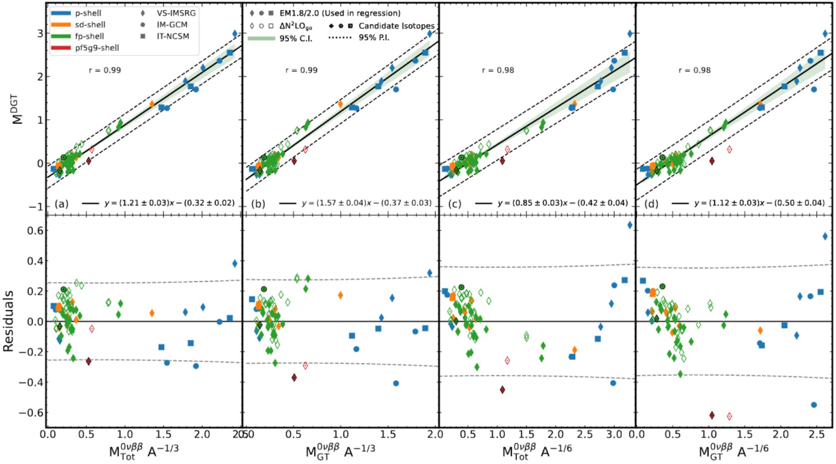

JMY et al., PRC106, 014315 (2022)

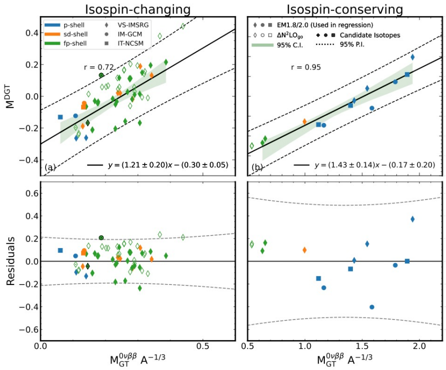

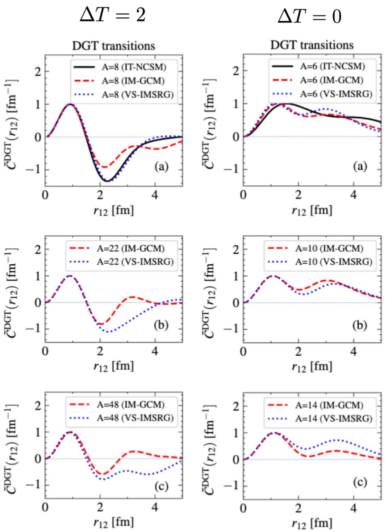

- The $0\nu\beta\beta$ and DGT of candidate nuclei are isospin-changing transitions (nodes).
- Cancellation results in weak linear correlation.

JMY et al., PRC106, 014315 (2022)

- Correlation relations from the VS-IMSRG calculation for ^{76}Ge-Se using 34 LECs samples of the Delta-full NNLO$_{\rm go}$(394) interaction.

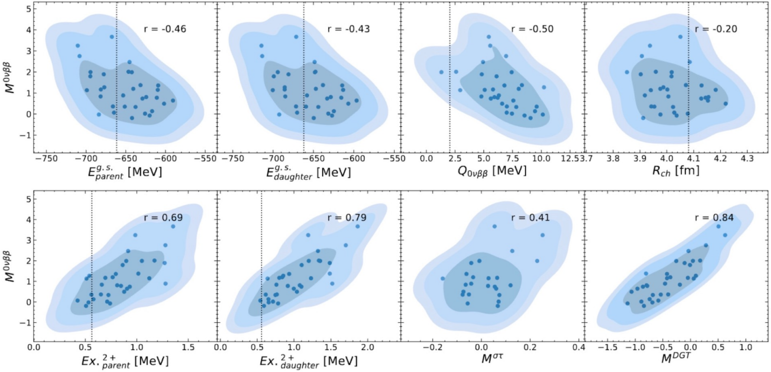

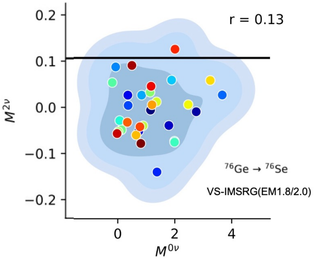

A. Belley et al., arXiv:2210.05809v1 [nucl-th]

ab initio correlation relation between NLDBD and LECs

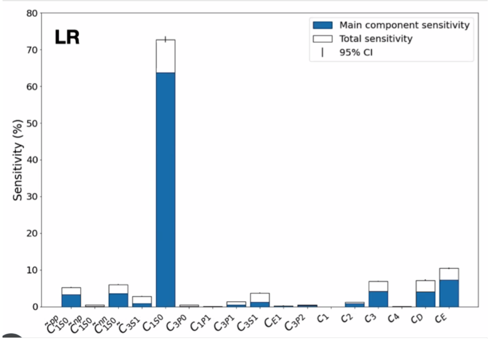

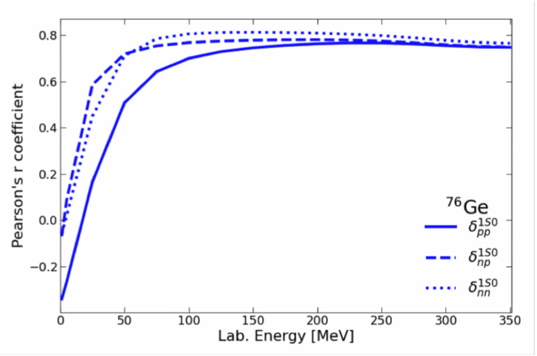

- The long-range part of the NME is sensitive to the LEC $C_{^1S_0}$.
- The phase shift of the $^1S_0(T = 1)$ channel is linearly correlated to the NME.
- The neutron-proton phase-shift δ_{np}^{1S0} at 50 MeV is used to weight the samples.

With both the long- and short-range transition operators, the VS-IMSRG method is applied to study the NMEs of heavier candidates:

- For ^{130}Te, $M^{0\nu}_{L+S} \in [1.52, 2.40]$
- For ^{136}Xe, $M^{0\nu}_{L+S} \in [1.08, 1.90]$

The uncertainty is composed of different sources: nuclear interaction, reference-state, basis extrapolation, closure approximation, and the LEC for the short-range transition operators.

The values are generally smaller than those from phenomenological nuclear models.

A more comprehensive quantification analysis

nuclear many-body truncation errors, convergence of NMEs with chiral expansion orders, etc.

A. Belley et al, arXiv:2307.15156 (2023)

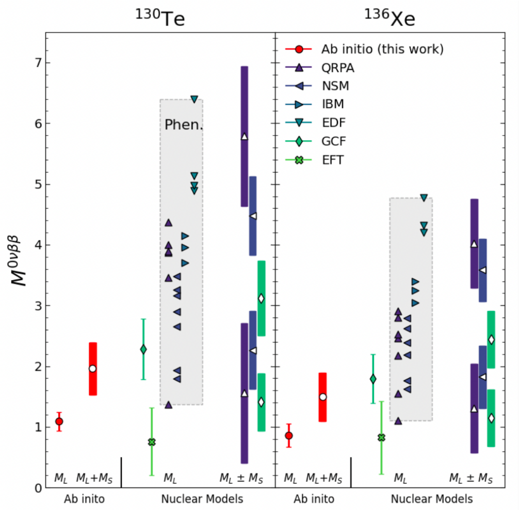

Convergence of the chiral expansion order for nuclear forces

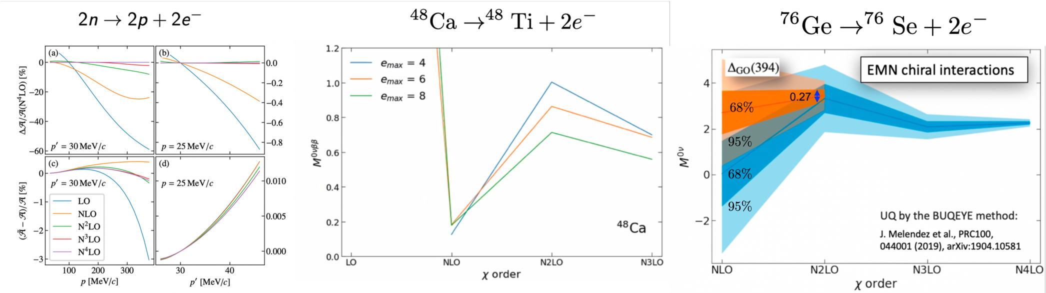

- The $\mathcal{A}_\nu(2n \to 2p + 2e^-)$ converges quickly w.r.t. the chiral expansion order of nuclear interactions.
- Convergence is slightly slower in ^{48}Ca, but much more rapid in ^{76}Ge.
- The uncertainty is also shrinking rapidly in ^{76}Ge.

- NME at the LO

$$\tilde{M}^{0\nu}_{\rm LO} = \tilde{M}^{0\nu}_{\rm LO,LR} + M^{0\nu}_{\rm LO,SR}.$$

$$\boxed{\tilde{M}^{0\nu}_{\rm LO,LR} = M^{0\nu}_{\rm LO,LR}(1,2,3) + M^{0\nu}_{\rm N2LO,LR}(4).}$$

- The NME (~0.08) at the N2LO is less than 5% of that at the LO.
- The uncertainty in the SR transition operator is about 0.13.
- The use of closure approximation: ~10% error.

Power counting

$$\nu = 2A + 2L - 2 + \sum_i \left(\frac{n_f}{2} + d - 2 + n_e\right)$$

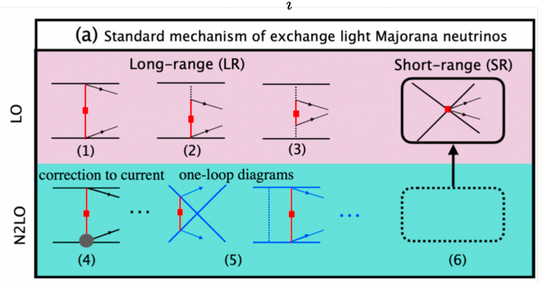

$e_{\rm Max}$	$M^{0\nu}_{\rm LO,LR}(1,2,3)$	$M^{0\nu}_{\rm LO,SR}$	$\tilde{M}^{0\nu}_{\rm LO,LR}$	$\tilde{M}^{0\nu}_{\rm LO}$	$M^{0\nu}_{\rm N2LO}(5)$
6	3.325	[0.872,1.152]	3.170	[4.04, 4.32]	0.196
8	2.092	[0.533,0.704]	2.020	[2.55, 2.72]	0.115
10	1.813	[0.437,0.577]	1.744	[2.18, 2.32]	0.090
extrap.	1.732	[0.399, 0.526]	1.670	[2.07, 2.20]	0.079

A. Belley, JMY et al, PRL132, 182502 (2024)

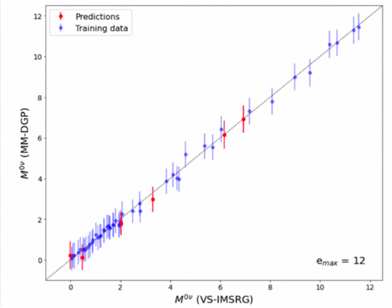

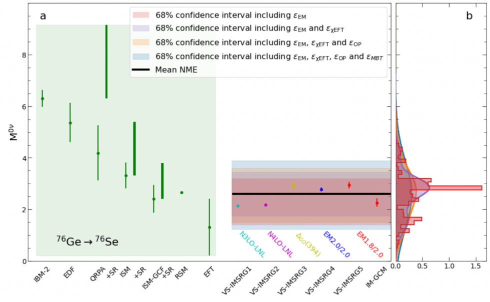

- Emulator, 8188 samples of chiral interactions, phase shift, $M^{0\nu} = 3.44^{+1.33}_{-1.56}$.
- Including the g.s. energies of $A = 2, 3, 4, 16$ and phase shift: $M^{0\nu} = 2.60^{+1.28}_{-1.36}$, which gives the effective neutrino mass $\langle m_{\beta\beta} \rangle = 187^{+205}_{-62}$ meV.
- The next-generation ton-scale Germanium experiment ($\sim 1.3 \times 10^{28}$ yr): $\langle m_{\beta\beta} \rangle = 22^{+24}_{-7}$ meV, covering almost the entire range of IO hierarchy.

A. Belley, JMY et al, PRL132, 182502 (2024)

$$\left(T_{1/2}^{0\nu}\right)^{-1} = \frac{1}{8\ln 2}\frac{1}{(2\pi)^5}\int \frac{d^3k_1}{2E_1}\frac{d^3k_2}{2E_2}|\mathcal{A}|^2 \times F(Z,E_1)F(Z,E_2)\delta(E_1+E_2+E_f-E_i),$$

where the total transition amplitude, V. Cirigliano et al., JHEP **12**, 097 (2018)

$$\mathcal{A} = \frac{g_A^2 G_F^2 m_e}{\pi R_A}\Big[\mathcal{A}_L \bar{u}(k_1) P_R C\bar{u}^T(k_2) + \mathcal{A}_R \bar{u}(k_1) P_L C\bar{u}^T(k_2) + \mathcal{A}_E \bar{u}(k_1)\gamma_0 C\bar{u}^T(k_2)\frac{E_1-E_2}{m_e} + \mathcal{A}_{m_e}\bar{u}(k_1) C\bar{u}^T(k_2) + \mathcal{A}_M \bar{u}(k_1)\gamma_0\gamma_5 C\bar{u}^T(k_2)\Big]$$

For each transition amplitude,

$$\begin{aligned}
\mathcal{A}_L &= \frac{m_{\beta\beta}}{m_e}\left(M_L^{I,NN} + M_L^{I,\pi N} + M_L^{I,\pi\pi}\right) + C_3^{II}\left(M_L^{II,\pi N} + M_L^{II,\pi\pi}\right) + C_{1L}^{III} M_L^{III,NN} + C_{2L}^{III} M_L^{III,\pi N} + C_{3L}^{III} M_L^{III,\pi\pi},\\
\mathcal{A}_R &= C_{1R}^{III} M_R^{III,NN} + C_{2R}^{III} M_R^{III,\pi N} + C_{3R}^{III} M_R^{III,\pi\pi},\\
\mathcal{A}_E &= C_1^{II} M_{E,1}^{II,NN} + C_2^{II} M_{E,2}^{II,NN},\\
\mathcal{A}_{m_e} &= C_1^{II} M_{m_e,1}^{II,NN} + C_2^{II}\left(M_{m_e,2}^{II,NN} + M_{m_e}^{II,\pi N} + M_{m_e}^{II,\pi\pi}\right),\\
\mathcal{A}_M &= C_{1M}^{III} M_M^{III,NN} + C_{2M}^{III} M_M^{III,\pi N}.
\end{aligned}$$

C R. Ding, G. Li, JMY, arXiv:2403.17722 [nucl-th] (2024)

Type−I

Type−II

Type−III

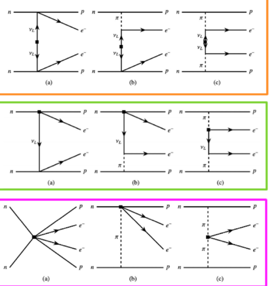

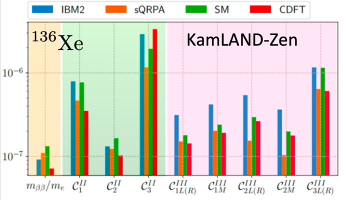

based on the assumption that the decay is driven by the operator of only one LEC.

The NMEs based on different mechanisms

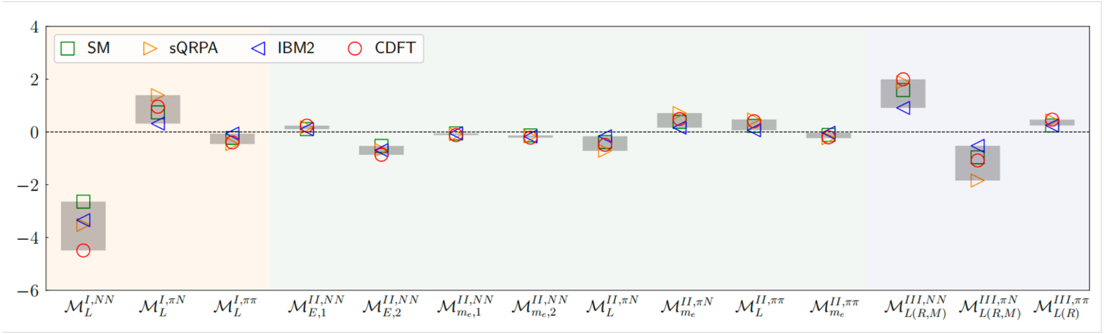

- Th NMEs for the type-I and III mechanisms are significantly larger than the Type-II mechanism (cancellation between different components of the NMEs).
- If the LECs for different mechanisms are at the same order, the standard mechanism and the short-range mechanism dominate the decay.

C R. Ding, G. Li, JMY, arXiv:2403.17722 [nucl-th] (2024)

Summary and perspective

- Remarkable advances have been achieved in studies of nuclear $0\nu\beta\beta$ decays, based on either phenomenological operators or operators from chiral EFT.
- Correlation relations between the NMEs of $0\nu\beta\beta$ decays and other observables have been extensively explored based on different models. With these correlations, uncertainty quantification has been carried out with the Bayesian analysis.
- A first such kind of analysis was carried out for ^{76}Ge, in which the NME turns out to converge rapidly with the chiral expansion order.

Next steps

- The NMEs of heavier candidates ^{82}Se, ^{100}Mo, ^{130}Te, ^{136}Xe, with reduced uncertainty: improve many-body truncation schemes, use higher-order operators, refine distributions of LECs, correct the contribution from the ultrasoft neutrinos (removing closure approximation).
- Ab initio studies of the contributions of nonstandard mechanisms.

Acknowledgements

SUN YAT-SEN UNIVERSITY

Collaborators

- SYSU
  C.R. Ding, C.F. Jiao, J.J. Liao, G. Li, C. C. Wang, X. Zhang
- PKU
  Lingshuang Song, Jie Meng, Peter Ring
- LZU: Yifei Niu
- CAEP: Bingnan Lv
- SWU: Longjun Wang
- MSU: S. Bogner, H. Hergert, R. Wirth
- UNC: Jonathan Engel, A. M. Romero
- TRIUMF: Antonie Belly, Jason Holt
- TU Darmstadt: Takayuki Miyagi
- Notre-Dame U: Ragnar Stroberg
- UAM: Benjamin Bally, Tomas Rodriguez

This work is supported in part by the National Natural Science Foundation of China (Grant Nos. 12141501 and 12275369), the Guangdong Basic and Applied Basic Research Foundation (2023A1515010936).

Thank you for your attention!

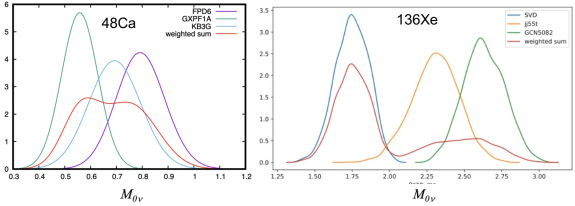

M. Horoi, A. Neacsu, S. Stoica, arXiv:2203.10577 [nucl-th]

- Bayesian Model Averaging of the probability distribution functions (PDF)

$$P(x = M^{0\nu}) = \sum_{m=1}^{3} W_m P_m(x),$$

- The weighted PDF is predominated by the model that reproduces the $M^{2\nu}$ (depending on the quenching factor q).
- With $q = 0.7$, the SVD model becomes predominant and $M^{0\nu} \in [1.55, 2.65]$ for ^{136}Xe with 90%C.L.

TABLE I. The rms deviations of the observables $E(0_1^+)$ (MeV), $E_x(2_1^+)$ (MeV), $B(E2: 0_1^+ \to 2_1^+)$ (e^2b^2) and R_p (fm) between the three types of emulators and the GCM calculations on the 32 testing points for ^{150}Nd and ^{150}Sm.

^{150}Nd	$\sigma[E(0_1^+)]$	$\sigma[E_x(2_1^+)]$	$\sigma[B(E2)]$	$\sigma[R_p]$
GCM(c_0)	5.9522	0.052	0.517	0.113
GCM(c_i^T)	0.2728	0.006	0.100	0.007
EC+GCM	0.2720	0.007	0.123	0.008
^{150}Sm				
GCM(c_0)	6.1291	0.081	0.505	0.106
GCM(c_i^T)	0.2875	0.186	0.154	0.093
EC+GCM	0.2717	0.040	0.212	0.007

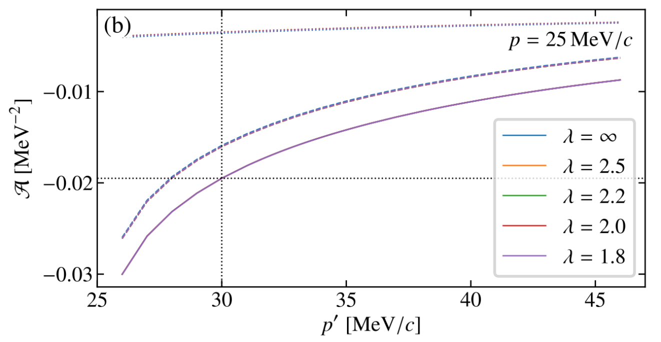

Figure: Momentum dependence of the short- and LO long-range parts, as well as the total amplitude for the EM potential at different SRG scales λ. Shown are the scaled short-range part $-2g_\nu^{NN}\mathcal{A}_S$ (dotted lines), the long-range part $\mathcal{A}_L$ (dashed lines), and the total amplitude $\mathcal{A}_L - 2g_\nu^{NN}\mathcal{A}_S$ (solid lines).

R. Wirth, JMY, H. Hergert, PRL127, 242502 (2021)

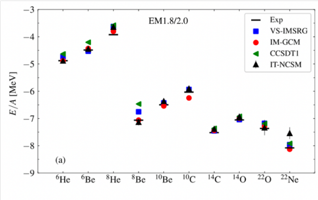

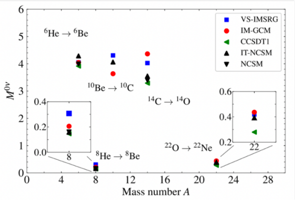

IM-GCM (EM1.8/2.0)

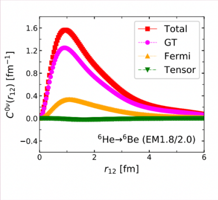

S. Pastore et al (2018)

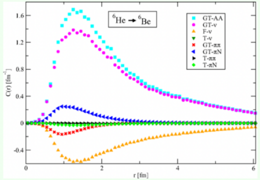

Note: A factor of $-g_A^2$ has been multiplied into the Fermi part.

JMY et al., PRC103, 014315 (2021)

- IT-NCSM and NCSM are quasi-exact methods, but limited to light nuclei.
- VS-IMSRG, IM-GCM, and CCSDT1 with some kinds of truncations can be applied to heavier candidate nuclei.
- Using different ab initio methods but the same input to estimate the truncation errors of the many-body methods.

Pairing fluctuation effect in MR-CDFT

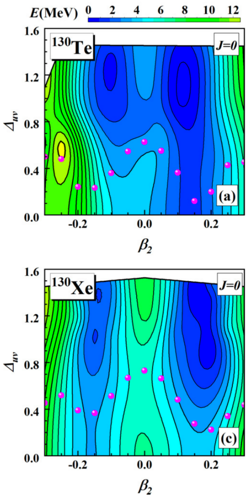

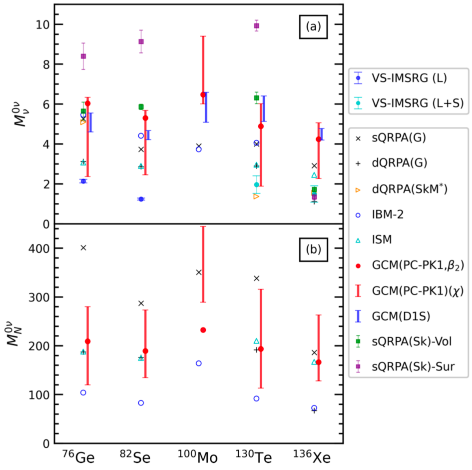

Ding, Zhang, JMY, Ring, Meng, PRC108, 054304 (2023)

The "magic" interaction EM1.8/2.0: The NN (N^3LO: D.R. Entem, R. Machleidt, PRC68 041001 (2003)) and local 3N interactions (N^2LO: K. Hebeler et al., PRC**83**, 031301(R) (2011)).

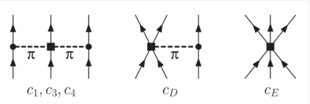

The LECs of the 3N are fitted on top of the SRG evolved NN interaction.

TABLE I. Results for the c_D and c_E couplings fit to $E_{^3\mathrm{H}} = -8.482$ MeV and to the point charge radius $r_{^4\mathrm{He}} = 1.464$ fm (based on Ref. [26]) for the NN/3N cutoffs and different EM/EGM/PWA c_i values used. For $V_{\mathrm{low}\,k}$ (SRG) interactions, the 3NF fits lead to $E_{^4\mathrm{He}} = -28.22\ldots-28.45$ MeV ($-28.53\ldots-28.71$ MeV).

	$V_{\mathrm{low}\,k}$		SRG	
Λ or λ/Λ_{3NF} (fm)	c_D	c_E	c_D	c_E
1.8/2.0 (EM c_i's)	+1.621	−0.143	+1.264	−0.120
2.0/2.0 (EM c_i's)	+1.705	−0.109	+1.271	−0.131
2.0/2.5 (EM c_i's)	+0.230	−0.538	−0.292	−0.592
2.2/2.0 (EM c_i's)	+1.575	−0.102	+1.214	−0.137
2.8/2.0 (EM c_i's)	+1.463	−0.029	+1.278	−0.078
2.0/2.0 (EGM c_i's)	−4.381	−1.126	−4.828	−1.152
2.0/2.0 (PWA c_i's)	−2.632	−0.677	−3.007	−0.686

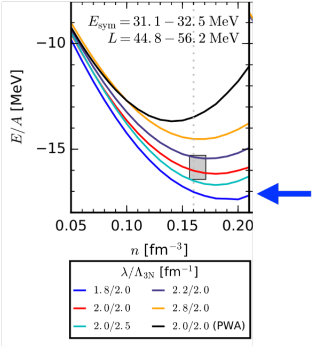

C. Drischler et al., PRL122, 042501 (2019)

The saturation properties are not well reproduced.

EFT: a model-independent analysis of operators at different energy scales

Cirigliano et al., JHEP (2018)

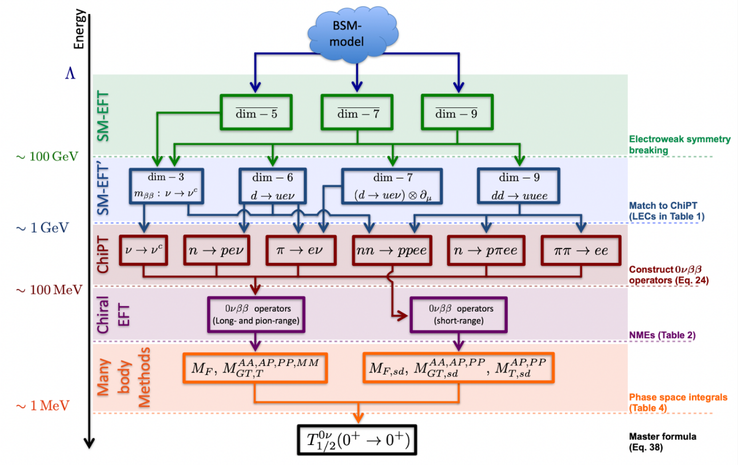

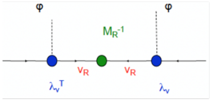

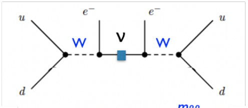

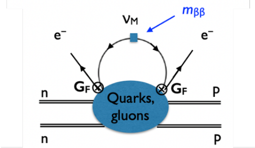

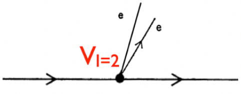

Emulating GCM with the EC: the Lipkin model

- The Hamiltonian of the Lipkin model

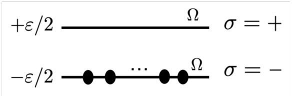

$$\hat{H} = \frac{\varepsilon}{2}\sum_{\sigma m}\sigma\hat{c}^{\dagger}_{\sigma m}\hat{c}_{\sigma m} - \frac{V}{2}\sum_{mm'\sigma}\hat{c}^{\dagger}_{\sigma m}\hat{c}^{\dagger}_{\sigma m'}\hat{c}_{-\sigma m'}\hat{c}_{-\sigma m}$$
$$= \varepsilon\hat{K}_0 - \frac{V}{2}(\hat{K}_+\hat{K}_+ + \hat{K}_-\hat{K}_-), \qquad \chi = \frac{V}{\varepsilon}(\Omega - 1)$$

- GCM wave function

$$|\Psi^{\kappa}_{\rm GCM}(\chi)\rangle = \sum_{\mathbf{q}=1}^{N_{\mathbf{q}}} f^{\kappa}(\chi;\mathbf{q})\,|\Phi(\mathbf{q})\rangle$$

$$|\Phi(\alpha,\varphi)\rangle = \prod_{m=1}^{\Omega} a^{\dagger}_{0m}(\alpha,\varphi)|-\rangle$$

- EC+GCM wave function

$$|\Psi^{k}_{\rm EC}(\chi_{\odot})\rangle = \sum_{\kappa=1}^{k_{\max}\geq k}\sum_{t=1}^{N_t} g^{k}(\kappa,\chi_t)\,|\Psi^{\kappa}_{\rm GCM}(\chi_t)\rangle$$

Generalized eigenvalue equation

$$\sum_{\kappa'=1}^{k_{\max}}\sum_{t'=1}^{N_t}\left[\mathcal{H}^{\kappa\kappa'}_{tt'}(\chi_{\odot}) - E^{k}_{\chi_{\odot}}\mathcal{N}^{\kappa\kappa'}_{tt'}\right]g^{k}(\kappa',\chi_{t'}) = 0,$$

QY Luo, X Zhang, LH Chen, JMY, arXiv:2404.08581

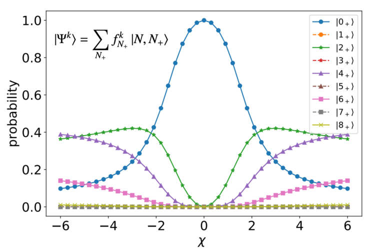

Diagonalization method

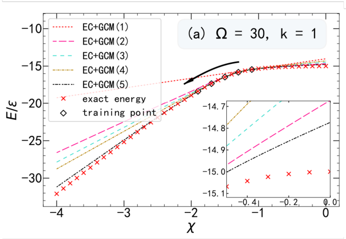

EC_1 +GCM

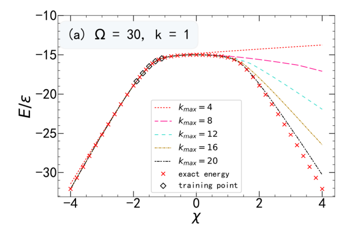

$\mathrm{EC}_{\mathrm{kmax}}$ +GCM

The missing piece in the LO transition operators

Featured in Physics | Editors' Suggestion | Open Access

New Leading Contribution to Neutrinoless Double-β Decay

Vincenzo Cirigliano, Wouter Dekens, Jordy de Vries, Michael L. Graesser, Emanuele Mereghetti, Saori Pastore, and Ubirajara van Kolck

Phys. Rev. Lett. **120**, 202001 – Published 16 May 2018

Physics See Synopsis: A Missing Piece in the Neutrinoless Beta-Dec

Nuclear force

Transition operator

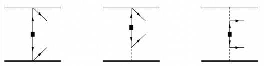

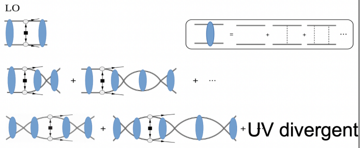

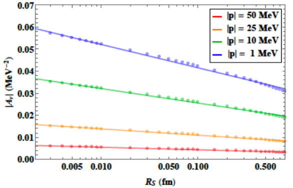

Lines fitted to $\mathcal{A}_\nu = a + b \ln R_S$

logarithmic dependence on R_S

Introducing a contact transition operator

$$V_{\nu,S} = -2 g_\nu^{NN} \tau^{(1)+} \tau^{(2)+}$$

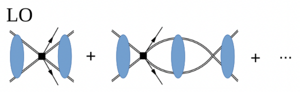

- The transition amplitude is regulator-dependent!
- Needs a counter term at LO in order to ensure renormalizability.

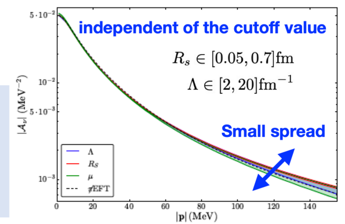

Toward Complete Leading-Order Predictions for Neutrinoless Double β Decay

Vincenzo Cirigliano, Wouter Dekens, Jordy de Vries, Martin Hoferichter, and Emar Mereghetti

Phys. Rev. Lett. **126**, 172002 (2021) – Published 30 April 2021

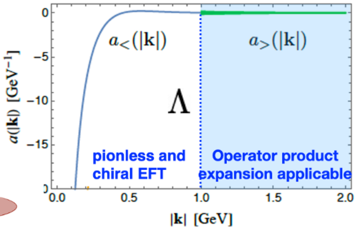

- **Cottingham formula** W.N. Cottingham, Ann. Phys. 25, 424 (1963)

$$\mathcal{A}_\nu \propto \int \frac{d^4k}{(2\pi)^4} \frac{g_{\mu\nu}}{k^2+i\epsilon} \int d^4x\, e^{ik\cdot x} \langle pp|T\{j^\mu_{\rm w}(x) j^\nu_{\rm w}(0)\}|nn\rangle$$

$$\mathcal{A}_\nu =$$

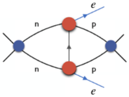

$$\propto \int \frac{d^4k}{(2\pi)^4} \frac{1}{k^2+i\epsilon}$$

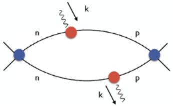

forward Compton amplitude

$$\mathcal{A}_\nu^{\rm full} = \int_0^\infty d|\mathbf{k}|\; a^{\rm full}(|\mathbf{k}|) = \mathcal{A}^< + \mathcal{A}^>\,,$$

$$\mathcal{A}^< = \int_0^\Lambda d|\mathbf{k}|\; a_<(|\mathbf{k}|)\,,$$

$$\mathcal{A}^> = \int_\Lambda^\infty d|\mathbf{k}|\; a_>(|\mathbf{k}|)\,,$$

- **Synthetic datum**

$$\mathcal{A}_\nu(|\mathbf{p}|,|\mathbf{p}'|) \times e^{-i(\delta_{^1S_0}(|\mathbf{p}|)+\delta_{^1S_0}(|\mathbf{p}'|))} = -\left(2.271 - 0.075\,\tilde{\mathcal{C}}_1(4\,M_\pi)\right) \times 10^{-2}\,\mathrm{MeV}^{-2}$$

$$\boxed{|\mathbf{p}| = 25\,\mathrm{MeV}\ (|\mathbf{p}'| = 30\,\mathrm{MeV})} \quad = -1.95(5)_{\tilde{\mathcal{C}}_1} \times 10^{-2}\,\mathrm{MeV}^{-2}\,,$$

Uncertainty from the estimate of the **inelastic** contributions

The transition amplitude is observable and thus scheme independent.

Low-lying states of ^{76}Ge-Se

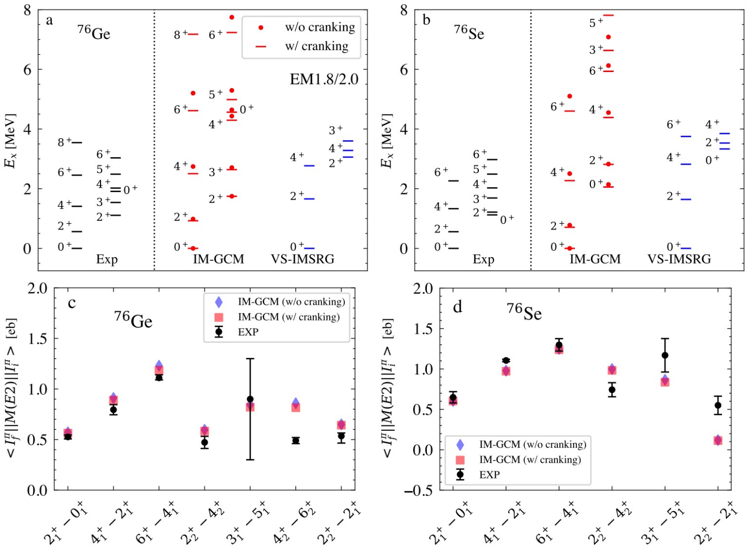

Research plans in China

Isotope	$G_{0\nu}$	$M^{0\nu}(\chi\mathrm{EFT})$	$T^{0\nu}_{1/2}$	$\langle m_{\beta\beta}\rangle$	Worldwide Exps	Inside China
	$[10^{-14}\ \mathrm{yr}^{-1}]$	[min, max]	[yr]	[meV]	current best limits	
76Ge	0.24	$2.60^{+1.27}_{-1.36}$	$> 1.8 \cdot 10^{26}$	187^{+205}_{-62}	GERDA: PRL125, 252502(2020)	CDEX
82Se	1.01		$> 4.6 \cdot 10^{24}$	.	CUPID-0: PRL129, 111801 (2023)	NvDEx
^{100}Mo	1.59		$> 1.5 \cdot 10^{24}$		CUPID-Mo: PRL126, 181802(2021)	CPUID-China
^{130}Te	1.42	[1.52, 2.40]	$> 2.2 \cdot 10^{25}$	[236, 373]	CUORE: Nature 604, 53(2022)	JUNO
^{136}Xe	1.46	[1.08, 1.90]	$> 2.3 \cdot 10^{26}$	[91, 160]	KamLAND-Zen: PRL130, 051801(2023)	PANDAX